

STRUCTURE OF THE CORE AND OF THE CENTRAL REGION OF AN EXTENSIVE AIR  
SHOWER AT SEA LEVEL

S. N. VERNOV, Ya. S. BABETSKIĬ, N. N. GORYUNOV, G. V. KULIKOV, Yu. A. NECHIN,  
Z. S. STRUGAL' SKIĬ, and G. B. KHRISTIANSEN

Nuclear Physics Institute, Moscow State University

Submitted to JETP editor August 13, 1958

J. Exptl. Theoret. Phys. (U.S.S.R.) **36**, 976-984 (April, 1959)

Experimental data on the lateral distribution of the energy flux of the electron-photon and nuclear-active components in the core and central region of extensive air showers are presented. It has been found that appreciable fluctuations in the lateral distribution of the energy flux of the electron-photon and nuclear-active components occur in the core of the showers and, apparently, in the central region as well. The data indicate the existence of a specific correlation between the lateral distribution of the energy flux of the electron-photon component and the lateral distribution of the energy flux of the nuclear-active component in an individual shower.

In a preceding article,<sup>1</sup> a new method of studying extensive air showers (EAS) has been described. It consists of a study of each recorded shower at various depths in its passage through dense matter, which, when the substance used is suitably chosen, makes it possible to observe the various shower components simultaneously.

The method had been applied to the study of the core of EAS, and preliminary experimental results were presented. A fuller report on the experimental data on the energy flux of the electron-photon and nuclear-active components of individual extensive air showers is given in the present article. The measurements were carried out by means of the array for comprehensive study of EAS, operating at Moscow State University.

## 1. EXPERIMENTAL SETUP

Data on the energy flux of the electron-photon and nuclear-active components were obtained by means of an array consisting of a large number of ionization chambers placed in two layers under composite absorbers made of lead and graphite. A detailed description of the chamber array is given in reference 1.

The use of an array consisting of a large number of ionization chambers of comparatively small dimension (25 cm) and covering a large area (4 m<sup>2</sup>) makes it possible to determine the position of the axis of each recorded shower with an error much smaller than the dimensions of the array. Thus, the array permits one to detect the passage of a shower axis through the array and

to investigate the phenomena accompanying such an event.\*

The position of the chamber array with respect to the hodoscope counters of the array for comprehensive study of EAS is shown in Fig. 1.

The presence of a large number of hodoscope counters both near the chamber array and at large distances from it make it also possible to use the chambers to obtain data on the energy flux of the electron-photon and nuclear-active components of EAS at large distances from the axis.

## 2. RESULTS OF MEASUREMENTS

During the time of operation of the ionization chamber array together with the full array (1800 hours), about 18,000 showers were recorded with a number of particles  $N$  in the range of  $10^3$  to  $10^6$ , and with the axis incident at distances up to 30 m from the ionization chamber array.

The experimental results obtained contain detailed data on the structure of each individually recorded shower. In view of the limited dimensions of the chamber array, most detailed data on the structure of an individual shower are ob-

\*An array of ionization chambers under an absorber has also been used for the study of high-energy nuclear-active component in reference 2. However, the setup used there was, for instance, not suitable for studying the correlation between the incidence of a shower axis on the array and the incidence of a high-energy nuclear-active particle, since the accuracy in determining the axis position from the hodoscope counters was of the order of the size of the chamber array.

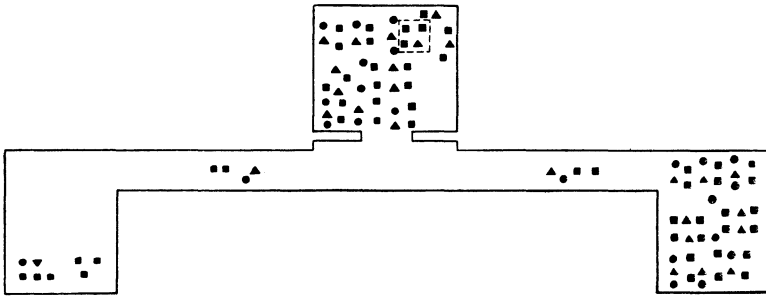


FIG. 1. Position of the ionization chamber array with respect to the hodoscope counters of the array for comprehensive study of EAS: ■ — trays of 12 counters with area  $330 \text{ cm}^2$  each; ▲ — trays of 24 counters with area  $100 \text{ cm}^2$  each; ● — trays of 24 counters with area of  $24 \text{ cm}^2$  each. The area occupied by the chamber array is denoted by the dashed line.

tained at comparatively small distances from the axis, in the so-called core region. The experimental results given below are deduced only from a part of available material.

The following method of selection of the cores of showers of various size was used. For the selection of shower cores of small-size showers, a systematical reduction of data obtained during 160 hours of operation of the array was carried out. With the selection system used (see reference 1), this corresponds to the recording of about 3000 events. The majority of these correspond to the passage of cores of showers of very small size, and also to the periphery of large showers. The ionization produced then in the first row of ionization chambers corresponds to the passage of a small number of relativistic particles and is comparable to the lower threshold of recording.

For the discussion to follow, we selected events where the ionization produced in the first row of chambers correspond to the passage of 200 and more relativistic particles through the volume of the chambers, and where the number of discharged hodoscope counters amounted to 20 out of 240 placed above the chamber array. A total of 146 such events was recorded. From these, events were then selected with a marked gradient of particle density over the first row of chambers and over the hodoscope counters placed near the chambers. Whenever in one, or in a few adjacent chambers, the ionization produced was larger than the ionization in neighboring chambers, and whenever an analogous region of maximum particle density was observed also by means of the hodoscope counters, then such an event was interpreted as an incidence of the axis of an extensive air shower upon the system. We found 55 such events, which correspond mainly to showers with a total number of particles  $N$  between  $6 \times 10^3$  to  $2 \times 10^4$ .

For the selection of the cores of EAS of medium size, the data obtained during another period of 170 hours of array operation was systematically reduced. These cases were considered where the ionization in the first row of chambers corre-

sponded to the passage of 500 and more relativistic particles and where the number of struck hodoscope counters amounted to 40 and more, out of 240 placed above the ionization chambers. In such a way, 40 events of incidence of EAS axes with total number of particles  $N$  between  $1.5 \times 10^4$  and  $4 \times 10^6$  were detected.

Finally, for the selection of the cores of showers of larger size, the data of the ionization chamber array obtained during 1000 hours of operation was analyzed systematically. Events were selected in which the ionization in the first row of chambers was larger than that corresponding to 2000 relativistic particles and where the EAS triggered the master system  $C_6$  (see reference 1). In this way, the incidence upon the ionization chamber system of 28 axes of EAS with total number of particles  $N$  from  $1 \times 10^5$  to  $2 \times 10^6$  was detected.

It should be noted that the above criteria for the selection of events in which a core of an EAS of a given size fell upon the ionization chamber array, are confirmed by a further detailed analysis of these events. In fact, as will be seen below, the ionization produced in the first row of chambers in the passage of the shower axes of a given size group was in all cases, many times smaller than that which was needed for the selection of showers of these size groups. As far as the requirement of the discharge of a given number of counters is concerned, it is determined by the required shower size under the assumption that the shower axis falls upon the ionization chamber array and that the lateral distribution of particle density is given by the standard function

$$\rho(r) \approx 2 \cdot 10^{-3} N / r \quad \text{for } r < 10 \text{ m.}$$

In order to obtain information on the energy flux at large distances from the shower axis, again only a part of the experimental data was used. Owing to the sharp decrease of the energy flux density with increasing distances from the axis, showers of sufficiently large size with a number of particles  $N > 10^5$  were chosen. For this purpose, data of the hodoscope counters were

TABLE I

$\Delta N$	$n$							
	<0.8	0.8-1.2	1.2-1.6	1.6-2.0	2.0-2.4	2.4-2.8	2.8-3.2	3.2-3.4
$1.0 \cdot 10^5 - 5.0 \cdot 10^5$	0	6	10	5	0	0	1	0
$1.5 \cdot 10^4 - 6.5 \cdot 10^4$	1	2	15	12	1	0	1	0
$5 \cdot 10^3 - 1.5 \cdot 10^4$	2	3	8	6	5	3	0	1
$5 \cdot 10^3 - 5 \cdot 10^5$	3	11	33	23	6	3	2	1

reduced for 190 hours of the operation of the array, and 300 showers with total number of particles  $N$  from  $10^5$  to  $10^6$  and with the axis falling at distances of up to 30 m from the ionization chamber array were selected. In the selection of a shower from the hodoscope data, the discharge of not less than 120 counters out of 240 placed above the ionization chamber array was required.

The recorded 130 events of incidence of the cores of EAS on the array were submitted to a detailed analysis, first from the point of view of the lateral distribution of the energy flux of the electron-photon component.

The flux of electrons and photons near the axes of the studied showers is so large that even for the least dense showers one should obtain a continuous distribution of ionization in the first row of chambers. For all 130 cases, the lateral distribution of ionization was constructed with respect to the point chosen as a shower axis, and under the assumption of a circular symmetry. This construction was carried out in the following way: In order to find the shower axis, the center of gravity method<sup>3</sup> was used. The indeterminacy in the position of the axis amounts then to the linear dimensions of a single chamber, i.e., to 25 cm. Concentric circles were drawn with the axis as center, forming a system of rings. Ionization in each ring was then computed. If a given ring contained only a part of a chamber, the contribution of the chamber was assessed in the following way: the ionization produced in the whole chamber was multiplied by the ratio of the area of the part belonging to a given ring to the area of the whole chamber. In order to obtain the energy flux density, the ionization was divided by the ring area. It should be noted that the most accurate distribution of the energy flux is obtained when the shower axis fell near the center of the chamber array since, in that case, one obtains a total azimuthal picture of the whole shower. This may be important for showers of small size in which the number of  $\pi^0$  mesons produced in the core is not so large as to ensure a circular symmetry of the shower.

In the majority of cases (90%) out of the 130

events analyzed, the distribution of the energy flux density can be represented by a single power law in the distance range under consideration

$$\rho_E(r) \sim r^{-n}.$$

The distribution of the exponents  $n$  is given in Table I, where a part of the reduced material is used (82 events).

It can be seen from the table that the lateral distribution of the energy flux of the electron-photon component near the shower axis is subject to large fluctuations; the exponent  $n$  assumes values from 1 to 3. It should be noted that the character of these fluctuations is identical for showers of different size.

The flux of nuclear-active particles is even near the shower axis insufficient to obtain a picture of the distribution of the high-energy nuclear-active component in the core of each individual shower. The lateral distribution of the energy flux of the nuclear-active component and the energy spectrum of nuclear-active particles in the shower core were therefore obtained statistically for several shower groups differing in the structure of the electron-photon component (see Table I). The lateral distribution of the energy flux of the nuclear-active component for two groups of showers ( $0.8 < n < 1.2$  — group 1;  $1.8 < n < 2.2$  — group 2) is given in Fig. 2.\* The average lateral distribution of the energy flux of the electron-photon component for these groups is also shown in the figure. A characteristic correlation in the form of these distributions may be observed; a slow decrease of the energy flux of nuclear-active component corresponds to a fast decrease of the energy flux of the electron-photon component with the distance from the axis, and vice versa for a slower decrease of electron-photon component, a faster decrease of the energy flux of the nuclear-active component is observed.

In connection with the above, it is of interest to compare the energy spectrum of nuclear-active

\*The position of the shower axis in the second row of chambers was determined from their position in the first layer, and from the angle of incidence (see reference 1).

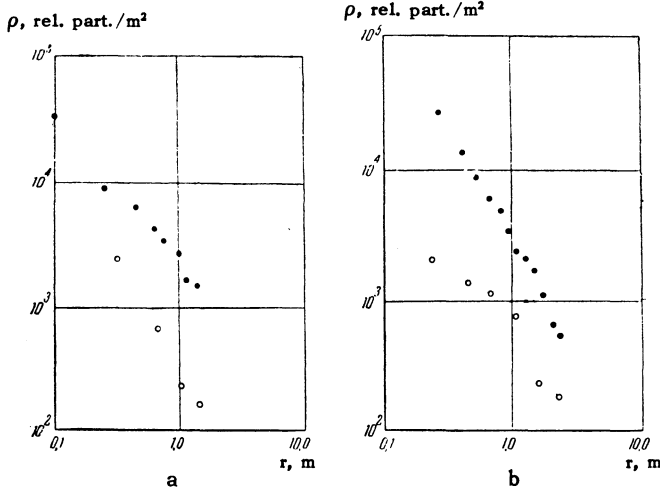


FIG. 2. Lateral distribution of the energy flux of the electron-photon and nuclear-active components in showers with different structure of the core: a - showers of group 1 for  $0.8 < n < 1.2$  (see Table I); ● - electron-photon component (slope  $\sim 1/r^{1.1}$ ); ○ - nuclear-active component (slope  $\sim 1/r^2$ ); b - showers of group 2: ● - electron-photon component (slope  $\sim 1/r^{1.9}$ ); ○ - nuclear-active component (slope  $\sim 1/r$ ).  $\bar{N} = 10^5$ , number of showers used - 8.

particles in the core of showers of the first and second groups. Corresponding data are shown in Fig. 3. The energy spectrum of nuclear-active particles in showers of both groups is found to be identical.\*

The 130 cases of incidence of a shower core upon the ionization chamber array discussed were further analyzed individually from the point of view of the absolute value of the energy flux contained in the core. The energy of the electron-photon component can be clearly determined for each individual case by the means of the following method: For each of the 130 showers, we have a lateral distribution of the energy flux density of the electron-photon component. In the majority of showers, the flux density is determined up to the distance of 1.5 m. We can therefore determine the energy flux of the electron-photon component in a circle with radius 1.5 m and with center coinciding with the shower axis for the majority of showers. The distribution of the absolute values of the energy flux is given in Fig. 4. It can be seen that the energy flux of the electron-photon component normalized to a given shower size is subject to marked deviations from the average value. This may be observed both in showers of the group 1 and in showers of the group 2 (the

\*It should be noted that the identification of high-energy nuclear-active particles from ionization bursts produced by them in the chambers was carried out taking into account the lateral divergence of particles over the area occupied by the chambers (for details, see reference 1).

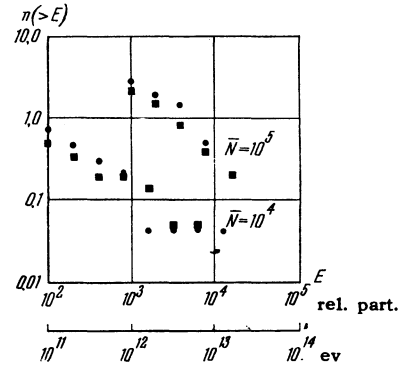


FIG. 3. Energy spectrum of nuclear-active particles in shower cores: ● - group 1 and ■ - group 2; x axis represents the energy of the nuclear-active particles expressed in the number of relativistic particles and in electron volts, the y axis represents the number of particles with energy larger than a given value in the core of showers with total number of particles indicated in the graph. In constructing the graph, it was assumed that the number of nuclear-active particles  $n(>E) \sim N$ , where  $N$  is the total number of particles in the shower.

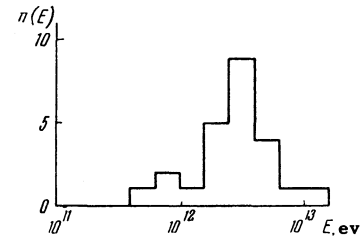


FIG. 4. Distribution of the absolute value of the energy flux of the electron-photon component in a circle with radius 1.5 m with center at the axis for showers with  $\bar{N} = 10^5$  (for groups 1 and 2 together). It was assumed that  $n(E) \sim N$ .

distributions were also constructed for separate groups).

A comparison of the average energy flux of the electron-photon component in the showers of the groups 1 and 2 is presented in Table II. It can be seen from the table that the average energy flux in the core is the same for the groups 1 and 2.

The determination of the absolute energy flux of the nuclear-active component in each individual shower, even in those of the largest size recorded, is difficult since the number of nuclear-active particles is small and the dimensions of the chamber array are comparable to the average deviation of these particles from the shower axis.

TABLE II

$\bar{N}$	Group	$E_{e-p}$ , ev	$E_{n-a}$ , ev	Number of showers
$1.0 \cdot 10^5$	1	$2.2 \cdot 10^{12}$	$5.0 \cdot 10^{12}$	8
	2	$3.3 \cdot 10^{12}$	$5.4 \cdot 10^{12}$	8
$1.0 \cdot 10^4$	1	$4.0 \cdot 10^{11}$	$1.7 \cdot 10^{12}$	11
	2	$5.0 \cdot 10^{11}$	$2.0 \cdot 10^{12}$	15

The average energy flux of the nuclear-active component for groups 1 and 2 was determined separately. These data are also given in Table II. It is found that the energy flux of the nuclear-active component in showers of the first and second groups is the same.

The correlation between the average energy flux of the nuclear-active component and the energy flux of the electron-photon component in the core is illustrated by Table III. The absolute value of the energy flux of the electron-photon component and the corresponding ratio of the burst size in the second layer to the burst size in the first layer of ionization chambers are given in the table. Group 1 comprises showers with an energy flux of the electron-photon component larger, and group 2 smaller, than the average. It can be seen that the energy flux of the nuclear-active component varies little with the change of the energy of the electron-photon component.

**TABLE III**

Group	Energy flux of the e-p component in a circle with radius $r = 1.5$ m $N = 10^5$	Ratio of the burst in the lower layer of chambers to the burst in the upper layer (shower axis within the limits of ionization chambers)
1 (11 showers)	$4.7 \cdot 10^4$	0.13
2 (12 showers)	$1.8 \cdot 10^4$	0.31

As has been mentioned above, because of the limited dimensions of the chamber array it was necessary to use a statistical approach, for the study of the structure of central regions of the showers at distances larger than 1.5 m from the axis. Data on the lateral distribution of the energy flux of the electron-photon component was obtained in such a way.

The 300 showers mentioned above with a number of particles  $N$  between  $10^5$  and  $10^6$  were used to obtain the distribution of the energy flux of electron-photon and nuclear-active components. Thanks to the large shower size, the comparatively large threshold of recording pulses from ionization chambers, equal to 5 to 10 relativistic particles, did not introduce any errors in the determination of the energy flux of the electron-photon components, even at distances up to 30 m. The flux of the energy of the nuclear-active component may, however, be underestimated because of the threshold.

The data obtained are shown in Fig. 5. Data on the lateral distribution of the energy flux in the shower core obtained for 28 showers of large size with  $N > 10^5$  particles (for  $r = 0.1 - 2$  m) are also shown in the figure.

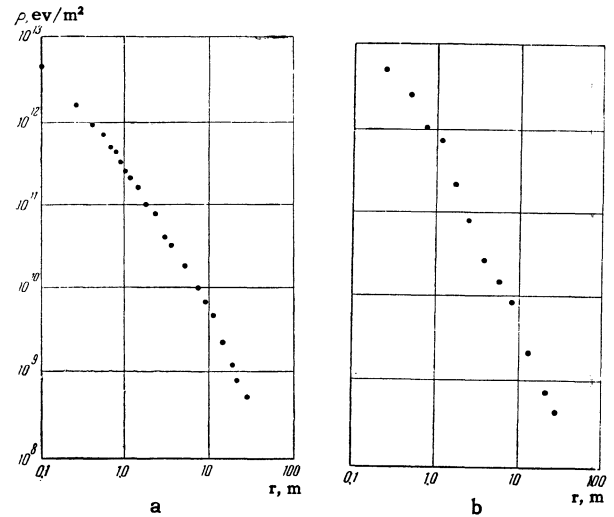


FIG. 5. Lateral distribution of the energy flux for showers with  $N = 10^5$  particles: a – electron-photon component in the distance range from 0.1 – 30 m; b – nuclear-active component in the distance range from 0.2 – 30 m.

The lateral distribution of the energy flux of the electron-photon components can be approximated by a power law

$$\rho_{E_{e-p}} \sim 1/r^{1.35} \text{ for } 0.1 \text{ m} < r < 2.0 \text{ m},$$

$$\rho_{E_{e-p}} \sim 1/r^2 \text{ for } 2.0 \text{ m} < r < 30 \text{ m}.$$

The lateral distribution of the energy flux of nuclear-active component can be given by the law

$$\rho_{E_{na}} \sim 1/r^2 \text{ for } 0.2 \text{ m} < r < 30 \text{ m}.$$

In order to find out to what degree the energy flux at large distances from the axis deviates from the average value, the distribution of the energy fluxes of the electron-photon component at a given distance from the shower axis was constructed, normalized to  $\bar{N}$ . This distribution is given in Fig. 6. It can be seen from the figure that the energy flux at a given distance from the axis deviates from the average flux much more markedly than it could be expected for Poisson fluctuations only.

### 3. CONCLUSION

The experimental data given above indicate clearly the presence of substantial fluctuations of the absolute energy flux of the electron-photon and nuclear-active components in the core of individual showers and in the lateral distribution of these fluxes. This fluctuation can be followed especially clearly for the electron-photon component. In a shower with a given total number of particles, the absolute value of the energy flux of the electron-photon component in the core can vary by an order of magnitude, and the distribution of the flux density can vary as  $1/r$  to  $1/r^3$ .

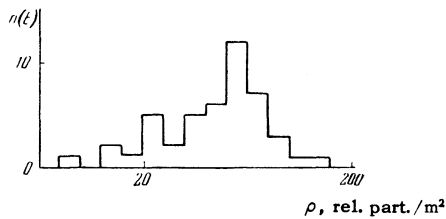


Fig. 6. Distribution of the absolute values of the energy flux of the electron-photon component at the distance of 10 m from shower axis with  $\bar{N} = 10^5$  particles. In constructing the distribution, it is assumed that  $n(E) \sim N$ .

It should also be noticed that fluctuations in the absolute value of the flux are independent of the fluctuations in the distribution of the flux density. This follows both from the direct considerations as well as from the value of the average energy of the electron-photon component in the core of EAS of groups 1 and 2, which are identical. Obviously, it is highly improbable that such fluctuations would be of a purely electromagnetic nature and were connected with the fluctuations in the development of the electron-photon cascade in air and the lead placed above the first row of chambers. These fluctuations must be naturally ascribed to the features of the nuclear cascade process.

The fluctuations of the ionization produced in the passage of the core of an individual shower observed in the second row of ionization chambers cannot obviously be interpreted directly as fluctuations in the energy flux of the nuclear-active component in the core. The reason is that fluctuations in the development of the nuclear cascade in the absorbers screening the second row of ionization chambers can be themselves sufficiently large, so that a different part of the energy of the nuclear-active particle will be transferred to the electron-photon component recorded by the chambers. On the other hand, as has been stated above, fluctuations are possible which are connected with the on the average comparatively large deviation of the nuclear-active high-energy particles from the shower axis. A statistical approach is therefore advisable.

As was seen from the data given in Sec. 2, in a shower with a given total number of particles  $N$ , the energy flux of the nuclear-active component is subject to fluctuations simultaneously with the energy flux of the electron-photon component, and the fluctuations of the lateral distributions of the energy flux of both components are connected by a definite correlation.

In showers of group 1, the lateral distribution of the energy flux of the nuclear-active component

is rather steep. In showers of group 2, a slow variation of the density flux is observed up to 1 m with a sharp decrease following. At the same time, the energy spectrum of the nuclear-active particles and the absolute energy flux of the nuclear-active component in the core are approximately the same for both groups.\*

In connection with the observed fluctuation and their features, a problem arises as to whether they exist only in the shower core, where a cascade consisting of a small number of high-energy particles is present, or whether they are characteristic of the shower as a whole. A direct observation of fluctuations in the energy flux density of the electron-photon component not only in the shower core but also at distances 10 m from the axis (see Fig. 6) shows that the second possibility seems to be very probable.

It should be noted that the above remark, as well as that about the correlation between the lateral distribution of the electron-photon and nuclear-active components, is based on the determination of the averages of the measured variables. The determination of the dispersion of the mean value can be carried out only by using a statistically large amount of material. Therefore, for a final solution of this problem, reduction of additional experimental material is necessary.

The authors would like to express their gratitude to G. T. Zatsepin and I. P. Ivanenko for valuable advice and discussion of results.

<sup>1</sup>Vernov, Goryunov, Zatsepin, Kulikov, Nechin, Strugal'skiĭ, and Khristiansen, J. Exptl. Theoret. Phys. (U.S.S.R.) **36**, 669 (1959). Soviet Phys. JETP **9**, 468 (1959).

<sup>2</sup>Dmitriev, Kulikov, and Khristiansen, Suppl. Nuovo cimento **8**, 587 (1958).

<sup>3</sup>Abrosimov, Goryunov, Dmitriev, Solov'eva, Khrenov, and Khristiansen, J. Exptl. Theoret. Phys. (U.S.S.R.) **34**, 1077 (1958); Soviet Phys. JETP **7**, 746 (1958).

Translated by H. Kasha

195

\*The total of experimental data cannot be explained without assuming the existence of a specific correlation in the angular distribution of  $\pi^0$  mesons and secondary nuclear-active particles in the elementary acts of the nuclear cascade process. It is namely necessary to assume that, for all small angular deviation of produced  $\pi^0$  mesons, a large angular deviation of the secondary nuclear-active particles with the energy of the same order occurs and vice versa. This problem, however, needs further detailed analysis.